Article

RNPS1 in PSAP complex controls periodic pre-mRNA splicing over the cell cycle

Kazuhiro Fukumura[1,*], Akio Masuda[2], Jun-ichi Takeda[2], Kinji Ohno[2] and Akila Mayeda[1,5,*]

[1]Division of Gene Expression Mechanism, Center for Medical Science, Fujita Health University, Toyoake, Aichi 470-1192, Japan

[2]Division of Neurogenetics, Center for Neurological Disease and Cancer, Nagoya University Graduate School of Medicine, Nagoya, Aichi 466-8550, Japan

[5]Lead Contact

*Correspondence:
fukumura@fujita-hu.ac.jp (K.F.), mayeda@fujita-hu.ac.jp (A.M.)

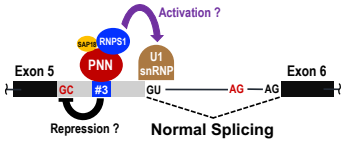

RNPS1 in PSAP Maintains Precise Splicing

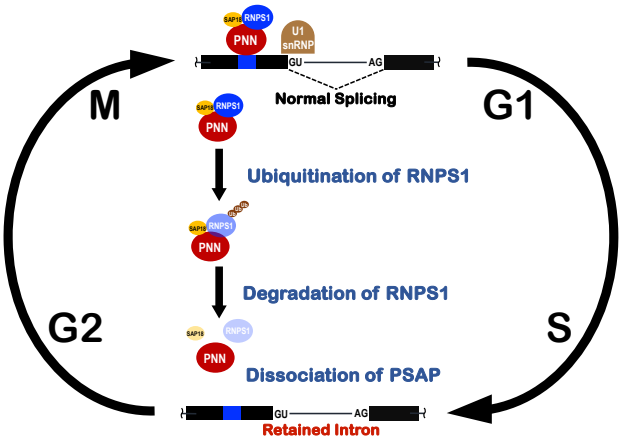

RNPS1 in PSAP Controls Cell Cycle-Dependent Splicing

Highlights

- The *AURKB* gene encodes a protein kinase essential for cytokinesis and cell cycle
- PSAP complex (RNPS1, PNN, SAP18) is required for precise splicing in *AURKB* intron 5
- RNPS1 protein in PSAP complex controls periodical splicing during the cell cycle
- Cyclical decrease of RNPS1 protein is mediated by the ubiquitin-proteasome pathway

SUMMARY

Cell cycle progression requires periodic gene expression through splicing control. However, the splicing factor that directly controls this cell cycle-dependent splicing remain unknown. Cell cycle-dependent expression of the *AURKB* (aurora kinase B) gene is essential for chromosome segregation and cytokinesis. We previously reported that RNPS1 is essential to maintain precise splicing in *AURKB* intron 5. Here we show that RNPS1 plays this role in PSAP complex with PNN and SAP18, but not in ASAP complex with ACIN1 and SAP18. Whole-transcriptome sequencing of RNPS1- and PNN-deficient cells indicated that RNPS1, either within or without PSAP complex, is an essential splicing factor for a subset of introns. Remarkably, protein expression of RNPS1, but not PNN, is coordinated with cyclical splicing in PSAP-controlled introns including *AURKB* intron 5. The ubiquitin-proteasome pathway is involved in the periodic decrease of RNPS1 protein level. RNPS1 is a key factor that controls periodic splicing during the cell cycle.

INTRODUCTION

Human pre-mRNA splicing takes place in the huge multimolecular complex, termed spliceosome, that is a highly organized dynamic ribonucleoprotein machine comprised of five snRNPs and numerous proteins (reviewed in Ref.[1,2]). While it is amazing to observe that each individual protein factor often drastically changes the outcome of splicing in a precisely regulated manner.

We originally identified human RNPS1 (RNA binding protein with serine-rich domain 1) as a general splicing activator *in vitro*[3]. We next found that RNPS1 exists in the spliceosome and regulates a variety of alternative splicing events, often collaborating with other splicing regulators, such as SRSF11 (p54), TRA2B (hTra2β), and PNN (PININ)[4,5]. RNPS1 was also identified as a peripheral factor of the exon junction complex (EJC) formed on spliced mRNA (reviewed in Ref.[6,7]).

ACIN1 (ACINUS) and PNN are scaffold proteins and form two alternative ternary complexes with RNPS1 and SAP18, termed ASAP and PSAP, respectively[8,9]. ACIN1 is involved in apoptosis and regulation of splicing and transcription[10-12] and PNN was originally identified as a desmosome-associated protein but also function as a regulator of alternative splicing[13,14].

Since ACIN1 bridges the ASAP complex to the EJC core[14] and PNN can be structurally replaced with ACIN1 to form PSAP[9], whole complexes of both ASAP and PSAP must interact with the EJC. Recent transcriptome-wide analysis indicated that the ASAP and PSAP complexes regulate distinct alternative splicing either in EJC core-dependent or -independent manner[14]. On the other hand, the EJC core alone, without any peripheral factors repress aberrant re-splicing on mature mRNA in cancer cells, implicating an important role in terminating splicing[15]. Many lines of evidence support that ASAP and PSAP complexes, with or without EJC core, are general regulators of splicing (reviewed in Ref.[7]). However, their

individual biological and physiological significance remains to be investigated.

We have been studying splicing regulation involved in mitotic cell-cycle progression using the *AURKB* (aurora kinase B) gene as a model. The *AURKB* gene encodes a serine/threonine protein kinase that is essential in chromosome segregation and cytokinesis during the cell cycle (reviewed in Ref.[16]). We previously showed that RNPS1, recruited by the EJC core, is critical for efficient and faithful splicing in mitotic cell cycle-related genes including *AURKB*[17]. Indeed, RNPS1 depletion causes a reduction of the AURKB protein due to multiple aberrant splicing, resulting in abnormal multinucleation phenotype that is fully rescued by ectopic expression of *AURKB*[18]. Regarding the mechanism of action, we found that RNPS1 protein binds directly to a specific element in exon 5 upstream of the authentic 5′ splice site, and this binding is critical to prevent multiple aberrant splicing using a common pseudo 5′ splice site[18]. Here we demonstrate that RNPS1 plays a role as the PSAP component in preventing aberrant splicing of *AURKB* pre-mRNA.

It was reported that SR protein kinase CLK1 (CDC-like kinase 1) controls many periodically spliced pre-mRNAs, including *AURKB*, during the cell cycle[19]. However, splicing factors were not known to be directly involved in cyclical splicing. Here we have discovered that the protein level of RNPS1 is coordinated with cell cycle-dependent periodic splicing of *AURKB* pre-mRNA. We propose a novel function of RNPS1 in PSAP complex, as a critical modulator that temporally controls periodic splicing observed during cell cycle.

RESULTS

PSAP promotes efficient and precise splicing of *AURKB* pre-mRNA

Previously, we reported that RNAi-mediated knockdown of RNPS1 induced aberrant splicing in the *AURKB* intron 5 and *MDM2* intron 10 (Figure S1A), and we identified the functional RNPS1 binding site upstream of the *AURKB* intron 5[18]. On the other hand, our previous yeast two-hybrid screening revealed that RNPS1 can bind to ACIN1, PNN, GPATCH8 and LUC7L3 (hLuc7A)[4]. This observation is consistent with the finding that ACIN1 and PNN form the ASAP and PSAP complex, respectively, with the common components RNPS1 and SAP18[8,9].

We then performed knockdown of all the components of the PSAP and ASAP complexes; i.e., RNPS1, ACIN1, PNN and SAP18. We confirmed that each siRNA led to effective depletion of the target mRNA and the protein product (Figure 1A). Notably, the knockdown of RNPS1, ACIN1 and PNN also caused co-depletion of SAP18 protein (left Western blot), however SAP18 mRNA levels were barely changed (right RT–PCR graph), indicating that SAP18 protein is stabilized in either ASAP or PSAP complex. Then, we examined whether these PSAP- and ASAP-components operate together with RNPS1 to ensure precise splicing in the *AURKB* intron 5 (Figure 1B) and the *MDM2* intron 10 (Figure S1B). We found that the knockdown of PNN and SAP18, as well as RNPS1, induced intron retention and aberrant splicing at expense of normal mRNA, but knockdown of ACIN1 did not. This confirms that the PSAP, but not ASAP, plays a role to restore the normal splicing in *AURKB* intron 5. The knockdown of other RNPS1-binding proteins, GPATCH8 and LUC7L3, barely affected in normal splicing (I) of the *AURKB* intron 5 and *MDM2* intron 10 (Figure S1B).

Previously, we demonstrated that RNPS1 binds to a specific *cis*-acting element (termed #3) located upstream of the authentic 5′ splice site of intron 5 (Figure 1C, upper scheme)[18]. We thus examined whether the PSAP complex binds to this *cis*-acting element. We transfected HEK293 cells with the AURKB/E5-WT or AURKB/E5-Δ#3 reporter mini-genes and performed RNA immunoprecipitation experiments using antibodies against each of the PSAP components (Figure 1C, lower panel). As we expected, RNPS1, PNN and SAP18 bound to the AURKB/E5-WT, but ACIN1 did not. Notably, deletion of this *cis*-acting element '#3' greatly reduced the binding of the PSAP components. We conclude that PSAP binding to the specific element '#3' is critical for efficient and precise splicing in the *AURKB* intron 5.

PSAP either represses the pseudo 5′ splice site or activates the authentic 5′ splice site in *AURKB* pre-mRNA

Since the '#3' element is located between the upstream pseudo 5′ splice site and the downstream authentic 5′ splice site, we postulated two conceivable mechanisms leading to the normal splicing; either (i) PSAP represses the pseudo 5′ splice site, and/or (ii) PSAP activates the authentic 5′ splice site (Figure S2A). To examine distance-dependent effects of PSAP binding, such as interaction with and/or steric hindrance to the U1 snRNP, we increased the distance of the '#3' element from either the authentic 5′ splice site or the pseudo 5′ splice site (Figure S2B).

These two variant *AURKB* pre-mRNAs, as well as the original *AURKB* pre-mRNAs, had equivalent repression of the normal 5′ splice site by the RNPS1-knockdown (Figure S2C), suggesting that both postulated mechanisms (see above) are involved. Several previous studies indeed support both possibilities (see DISCUSSION).

Individual subsets of introns are spliced out by RNPS1, PNN and PSAP

To test whether PSAP might have a general role in controlling splicing, we performed RNAi-mediated knockdown of RNPS1 and PSAP-specific component PNN in HEK293 cells and the total RNA was analyzed by whole-transcriptome sequencing (RNA-Seq). The sequencing reads from the RNPS1- and PNN-deficient cells were mapped to the human genome and we analyzed intron retention as a consequence of splicing defect.

We identified a total of 131 overlapping events of intron retention in the RNPS1- and PNN-deficient cells (Figure 2A, Table S2), indicating that 131 introns are PSAP-dependently spliced. The data also indicate that RNPS1 and PNN solely (not in PSAP complex) promote splicing in 791 and 53 introns, respectively. We validated the PSAP-dependent splicing defect by RT–PCR with three representative PSAP-controlled introns (arbitrarily chosen from 131 introns in Table S2). By depletion of PSAP components (RNPS1 and PNN), we observed intron retention in all these introns, but not in the control authentic *ACTG1* intron 3 (Figure 2B). We conclude that PSAP function as a general splicing factor in a subset of introns.

RNPS1 in PSAP controls periodic splicing over the cell cycle

A previous RNA-Seq analysis at different stages of the cell cycle identified ~1300 genes with changes of cell cycle-dependent alternative splicing, and interestingly, the intron retention

event of *AURKB* intron 5 was characterized as a representative model[19]. The excision of *AURKB* intron 5 was periodically modulated and this splicing activity reaches the maximum around M phase (Figure 3A). Using the same *AURKB* pre-mRNA including intron 5, we found that RNPS1 in PSAP complex controls its precise splicing (Figure 1)[18]. Therefore, we hypothesized that PSAP also plays a role in cell cycle-dependent splicing observed in *AURKB* intron 5.

We first recapitulated the periodic splicing of *AURKB* intron 5 during cell cycle progression with HEK293 cells (Figure 3B). We treated the cells with the microtubule-destabilizing reagent, nocodazole, which arrests cells cycle at the start of the G2/M phase (nocodazole release 0 h). Using RT–PCR and quantitative RT–PCR (RT–qPCR), we observed increased intron 5 retention from G2/M to G1/S phase (nocodazole release 4–8 h). On the other hand, we found decreasing intron 5 retention from G1/S to G2/M phase in synchronized HEK293 cells after release from the double thymidine block at the G1/S boundary (Figure S3).

It was important to confirm whether the observed cyclical splicing modulation is a general event in all the PSAP-controlled introns. Using three representative PSAP-controlled introns (Figure 2A), we examined the changes in intron retention events during the cell cycle using nocodazole and double thymidine to synchronize HEK293 cells (Figure 3C, Figure S3). Remarkably, in these PSAP-controlled introns, we also observed periodic changes in the intron retention as observed in *AURKB* intron 5 pre-mRNA (Figure 3B, Figure S3). Our results thus provided the mechanistic basis to the reported periodical pattern of splicing activity (Figure 3A). Here we propose that PSAP promotes periodic splicing linked to the cell cycle.

Periodic decrease of RNPS1 protein is mediated by the ubiquitin-proteasome pathway

We assumed that PSAP-controlled periodic splicing was modulated by the expression level changes of PSAP components. We thus examined the protein levels of PSAP components during the cell cycle using nocodazole synchronized HEK293 cell (Figure 4A, left panel). Intriguingly, RNPS1 protein level was at a maximum in G2/M phase (nocodazole release 0 h) and decreased through cell cycle progression (nocodazole release 4–8 h), and then started to increase again (nocodazole release 12 h). This periodic change in RNPS1 protein was coordinated with the level of AURKB protein, which was at a high level in G2/M and declined to a low level in G1/S by degradation (Figure 4A, left panel)[20]. In contrast, protein levels of other PSAP components PNN and SAP18, as well as an ASAP component ACIN1, were barely changed. Notably, we did not observe such a periodic change in RNPS1 mRNA expression level during cell cycle (Figure 4A, right graph) as previously observed in human RNPS1 (E5.1)[21]. These data together indicate that the reduction of RNPS1 protein level is regulated at the protein level, but not at the mRNA level.

We also performed the same experiments using the double thymidine block synchronized HEK293 cells (Figure 4B, left panel). We found that RNPS1 protein was minimal at G1/S phase (double thymidine release 0 h) and increased as the cell cycle progressed to G2/M phase (double thymidine block 4–12 h). The protein expression of ACIN1, PNN, and SAP18 were also somewhat increased. These results could be partly due to the mRNA level of PSAP

components, RNPS1 and PNN, were increased, together with AURKB, from G1/S into G2/M phase (Figure 4B, right graph).

Since RNPS1 and AURKB protein expressions were synchronized during the cell cycle (Figure 4A, B, left panels), we assumed that RNPS1, but not other PSAP components, was responsible for the observed cell cycle-dependent splicing modulation (Figures 3B, C; Figure S3). To test this assumption, we performed nocodazole treatment in RNPS1-knockdown HEK293 cell (Figure S4A) and analyzed intron retention events in the two PSAP-controlled introns (Figure S4B). We observed that RNPS1-knockdown induced the intron retention even at the RNPS1-upregulated G2/M phase. We conclude that RNPS1, as a component of the PSAP, promotes the periodic pre-mRNA splicing linked to cell cycle progression.

Ubiquitin-mediated proteolysis is one of the keys to cell cycle progression[22]. RNPS1 is polyubiquitinated by K48-linkage and degraded by the proteasome[23]. Therefore, we assume that periodical degradation of RNPS1 protein is controlled by ubiquitin-proteasome pathway. We treated HEK293 cells with proteasome inhibitor MG132 and we examined the protein level of PSAP components. As we expected, RNPS1 protein was stabilized in the presence of MG132 whereas the level of other ASAP/PSAP proteins, ACIN1, PNN and SAP18, were not changed at all (Figure 4C). Since the degradation of RNPS1 causes co-destabilization of SAP18 (Figure 1A), the functional PSAP complex appears to be dissociated that induces eventual intron retention. Taken together, we conclude that ubiquitin-proteasome pathway plays a key role in the periodic fluctuation of RNPS1 protein level, leading to observed periodic splicing in accordance with the cell cycle (Figure 5).

DISCUSSION

The PSAP complex as a splicing factor is critical to maintain splicing fidelity

We previously reported that RNPS1 interacts with a specific *cis*-element and ensures precise splicing in the *AURKB* pre-mRNA, which is essential for chromosome segregation and cytokinesis[18]. Here, we demonstrate that RNPS1, as a component of PSAP with PNN and SAP18, binds to the same *cis*-element in the upstream exon, leading to the precise splicing on *AURKB* intron 5 (Graphical Abstract, upper panel).

The PSAP components (PNN, SAP18 and RNPS1) are all associated with the EJC core as peripheral factors (reviewed in Ref.[6,7]). Therefore, it is conceivable that the EJC recruits the PSAP complex on the target pre-mRNA and PSAP itself functions to promote precise splicing. Indeed, we previously found that EJC core on pre-mRNA recruits RNPS1 as a key factor and it promotes splicing involved in mitotic cell cycle[17].

Regarding the mechanism of PSAP-mediated control to ensure precise splicing in *AURKB* pre-mRNA, our data implicate that it occurs either through repression of the upstream pseudo 5′ splice site (without direct masking) or through activation of the downstream authentic 5′ splice site, likely through the interaction with U1 snRNP (Figure S2A; see 'Limitations of the study'). Since the downstream authentic 5′ splice site is much weaker than the upstream pseudo 5′ splice site[18], the intrinsic RNPS1 activity as a general splicing activator [3], in a component of PSAP, must be a prerequisite for the use of the weak authentic 5′ splice site.

On the other hand, repression of the pseudo 5′ splice site cannot be ruled out since RNPS1-knockdown produces five aberrant mRNAs using a common upstream pseudo 5′ splice site and the downstream five 3′ splice sites in endogenous *AURKB* pre-mRNA[18]. This 'repression' scenario is consistent with two recent observations that EJC-recruited PSAP represses distant pseudo and recursive 5′ splice site[24,25], however, the underlying mechanism to repress such distant 5′ splice site without a steric hindrance remains unknown.

A novel RNPS1 function in periodical splicing during the cell cycle

Cyclical removal of *AURKB* intron 5 contributes to periodic AURKB protein expression during the mitotic cell cycle[19]; however, the involved mechanism remains to be elucidated. Our finding may provide a breakthrough in addressing this important open question. Here we propose that splicing activator RNPS1 in PSAP complex not only functions to ensure precise splicing, but also plays an essential role in controlling periodic splicing linked to cell cycle (Graphical Abstract, lower panel).

Our whole-transcriptome sequencing (RNA-Seq) analysis in RNPS1- and PNN-knockdown cells showed that most affected splicing events were intron retentions, and our arbitrarily chosen intron retention events were all induced from G2/M phase to G1/S phase as observed previously in *AURKB* intron 5[19]. We eventually discovered that the level of RNPS1 protein is down-regulated in G1/S phase by the ubiquitin proteasome pathway and it is gradually up-regulated to its maximum level at M phase. This characteristic temporal fluctuation of the RNPS1 protein level is well accounted for by the periodic splicing in accordance with the cell cycle (Figure 5). Since the protein levels of other PSAP components, PNN and SAP18, remain constant during the cell cycle, it is likely that the functional PSAP complex is dissociated by the lack of RNPS1 component.

Previously, it was reported that knockdown of EJC-core component, RBM8A (Y14), induces abnormal nuclear structure, multinucleated cells, G2/M cell cycle arrest, and genome instability (Ref.[17,26]; and references therein), which is a similar phenotype to that caused by the knockdown of PSAP component, RNPS1[18]. In mouse models, it was reported that haploinsufficiency of MAGOH, the other EJC core component, causes the defect of mitosis of neural stem cells, ending up in microcephaly[27]. Together, it is very likely that the EJC recruits the functional PSAP complex on the cell cycle-dependently spliced pre-mRNAs, as well as on the pre-mRNAs to ensure splicing fidelity.

We demonstrate that PSAP, but not ASAP, controls the faithful splicing and alternative splicing of transcripts involved in the mitotic cell cycle. Therefore, the function of these two complexes is determined by only one distinct component of PSAP and ASAP, i.e., PNN and ACIN1 (Figure 1A, top schemes). Consistently, a recent report showed that PSAP and ASAP form functionally distinct complexes with the EJC core to confer distinct alternative splicing activities[14]. On the other hand, since RNPS1 is a common component of PSAP and ASAP, periodic changes of RNPS1 protein would also be expected to modulate the function of ASAP during the cell cycle. Indeed, a possible function of ASAP in the cell cycle is suggested by the fact that depletion of the component of ASAP, ACIN1, cause defects in cell cycle progression[28]. Moreover, the genome-wide identification of RNA targets suggests the role of

ACIN1 in cell cycle[12]. Taken together, we speculate that PSAP and ASAP complexes may target distinct subsets of pre-mRNAs and control periodic changes of splicing during the cell cycle. Although it is out of scope for this article, there is considerable interest in identifying these distinct subsets of pre-mRNAs.

Limitations of the study

We previously found that RNPS1 can bind to a component of U1 snRNP, LUC7L3 (one of the human paralogs of yeast Luc7A)[4]. It was also shown that LUC7L3 overexpression changes the selection of the alternative 5′ splice site *in cellulo*[29]. We thus tested our hypothesis that the weak authentic 5′ splice site is activated through RNPS1 binding to LUC7L3 in the U1 snRNP. However, depletion of LUC7L3 has no effects on the PSAP-dependent *AURKB* and *MDM2* pre-mRNA splicing (Figure S1B), suggesting that RNPS1–LUC7L3 interaction is not involved in these two PSAP-dependent splicing events. Of course, we cannot rule out the possibility of RNPS1 interaction with other U1 snRNP components. Interestingly, recent study showed that three human paralogs, LUC7L, LUC7L2 and LUC7L3, as components of the U1 snRNP, regulates unique alternative splicing profiles[30].

Further studies are needed to elucidate the PSAP-mediate molecular mechanism to ensure splicing fidelity.

MATERIALS AND METHODS

Cultures of human cells

HeLa and HEK293 cells were cultured in Dulbecco's modified Eagle's medium (DMEM; Wako) supplemented with 10% fetal bovine serum (Sigma-Aldrich) and 1% penicillin-streptomycin (Nakarai Tesque). Cells were grown at 37°C in 5% CO_2.

Construction of expression plasmids

The pcDNA3-Flag-RNPS1 expression plasmid was described previously[18]. To construct the expression plasmids, pcDNA3-AURKB/E5-WT and the pcDNA3-AURKB/E5-Δ#3, the fragments containing the 3′ end of intron 4, exon 5 and the 5′ end of intron 5 were amplified by PCR from pcDNA3-AURKB/E5-E6 and pcDNA3-AURKB/E5-E6-Δ#3 plasmids[18], respectively, and these were subcloned into pcDNA3 vector (Invitrogen–Thermo Fisher Scientific). The pcDNA3-AURKB/E5/inR-E6 and pcDNA3-AURKB/E5/inL-E6 plasmids were constructed using overlap extension PCR as previously described[31]. All PCRs were performed with PrimeSTAR Max DNA Polymerase (Takara Bio) using the described primer sets (Table S1).

RNAi-mediated knockdown and splicing assay

The transfection of HeLa and HEK293 cells with siRNAs (100 pmol each) was performed using Lipofectamine RNAi max (Invitrogen-Thermo Fisher Scientific) according to manufacturer's protocol. The siRNAs targeting RNPS1, ACIN1, PNN, SAP18, GPATCH8 and LUC7L3 (Table S1) were purchased (Nippon Gene).

At 72 h post-transfection, total RNAs were isolated from HeLa and HEK293 cells using the

NucleoSpin RNA kit (Macherey-Nagel). To examine endogenous mRNA expression levels and the splicing products, total RNAs were reverse transcribed using PrimeScript II reverse transcriptase (Takara Bio) with oligo-dT and random primers, and the obtained cDNAs were analyzed by PCR and quantitative PCR (qPCR) using specific primer sets (Table S1).

All primers oligonucleotides were purchased (Fasmac) and all PCRs were performed with Blend Taq polymerase (Toyobo). The PCR products were analyzed by 6% polyacrylamide gel electrophoresis (PAGE). PCR products of aberrantly spliced and intron retained mRNAs were quantified using NIH Image J software. Eco Real-Time PCR system (Illumina) was used for qPCR analysis with Thunderbird SYBR qPCR Mix (Toyobo). All the experiments were independently repeated three times. Mean values, standard error of the mean (SEM), and Welch's *t*-test were calculated using Excel (Microsoft).

Western blotting analysis

At 72 h post-transfection, total protein was isolated from siRNA-treated HeLa and HEK293 cells to examine the endogenous protein expression levels. Cells were suspended in Buffer D [20 mM HEPES (pH 7.9), 50 mM KCl, 0.2 mM EDTA, 20% glycerol], sonicated for 20 sec, centrifuged to remove debris, and the lysates were subjected to Western blotting. The procedure, detection and analysis were described previously[31].

The following antibodies were used to detect target proteins: anti-RNPS1 (1:750 dilution)[3], anti-ACIN1 (1:1500 dilution; Cells Signaling Technology), anti-PNN (1:1500 dilution; Sigma-Aldrich), anti-SAP18 (1:1500 dilution; Proteintech), anti-AURKB (1:1500 dilution; Cells Signaling Technology) and anti-GAPDH (1:1500 dilution; MBL Life Science) antibodies.

RNA immunoprecipitation assay

HeLa cells (in 60-mm dishes) were co-transfected with pcDNA3-Flag-RNPS1 and pcDNA3-AURKB/E5-WT or the pcDNA3-AURKB/E5-Δ#3 using Lipofectamine 2000 (Invitrogen–Thermo Fisher Scientific). After culturing for 48 h, whole cell extracts were prepared and mixed with each antibody conjugated with Dynabeads Protein A (Invitrogen–Thermo Fisher Scientific). After culturing for 48 h, whole cell extracts were prepared and mixed with each antibody) in NET2 buffer [50 mM Tris (pH 7.5), 150 mM NaCl, 0.05% Nonidet P-40]. After 3 h incubation at 4°C, the beads were washed six times with NET2 buffer and bound RNA was eluted by TRI Reagent (Molecular Research Center). The precipitated RNAs were reverse transcribed by PrimeScript II reverse transcriptase (Takara Bio) with SP6 primer, and qPCRs were performed using specific primer sets (Table S1).

High-throughput RNA sequencing (RNA-Seq) analysis

The RNA libraries were prepared from three RNA sources; HEK293 cells transfected with siRNAs targeting RNPS1 and PNN (with control siRNA). mRNA isolation, cDNA library construction and whole-transcriptome sequencing was performed by Macrogen Japan Corporation.

The obtained reads were mapped to the human genome as follows. FASTQ files were filtered by Trimmomatic v0.36[32] with the parameters "PE-phred33

ILLUMINACLIP:Trimmomatic-0.36/adapters/TruSeq3-PE.fa:2:30:10 LEADING:3 TRAILING:3 SLIDINGWINDOW:4:15 MINLEN:150" and trimmed by fastx_trimmer included in the FASTX-Toolkit v0.0.13 (http://hannonlab.cshl.edu/fastx_toolkit/index.html) with the parameter "-l 150". The qualified FASTQ files were mapped to human genome hg19 by TopHat v2.1.1[33] and the transcripts were assembled by Cufflinks v2.2.1[34] with default parameters. PSI (percent-spliced-in) values were estimated by MISO v0.5.2[35] using the assembled transcripts as previously described[36].

The raw data derived from RNA-Seq analysis (see Figure 2A) have been deposited in DDBJ database and are publicly available as of the date of publication (Accession number: DRA016802).

Cell cycle synchronization experiments

To achieve cell synchronization at G2/M phase, HEK293 cells were plated (in 35-mm dishes) at 40% confluency. Cells were subsequently treated with 2 mM thymidine (Sigma-Aldrich) for 24 h, washed with PBS, and supplemented with fresh DMEM. After culture for 3 h, cells were followed by 12 h culture in the presence of microtubule-disrupting agent nocodazole at 100 μM concentration (Sigma-Aldrich). To remove nocodazole, cells were washed with phosphate-buffered saline (PBS) and cultured in fresh DMEM. Cells were harvested every 4 h for 12 h after the removal of nocodazole.

To achieve cell synchronization at G1/S phase, HEK293 cells were plated (in 35 mm dishes) at 20% confluency. Cells were treated with 2 mM thymidine for 18 h, washed with PBS, and supplemented with DMEM. After culture for 9 h, cells were treated with 2 mM thymidine for another 15 h. Cells were released from thymidine block by washing with PBS followed by culture in fresh DMEM. Cells were harvested every 4 h for 12 h after the removal of thymidine.

To inhibit proteasome, HEK293 cells were treated with MG132 (Sigma-Aldrich) at a final concentration of 1 or 10 μM. After 16 h of culture, cells were harvested and total protein was isolated (see above).

Quantification and statistical analysis

Three independent experiments were performed. Mean values, SE values, and Welch's t-test were calculated using Excel (Microsoft).

ACKNOWLEDGEMENTS

We thank H. Shirasaki and T. Kanehisa for technical support, and members of our labs for constructive discussions.

K. Fukumura was partly supported by Grants-in-Aid for Scientific Research (C) [Grant numbers: JP18K07304, JP21K07202] from the Japan Society for the Promotion of Science (JSPS), a Research Grant from the Hori Sciences and Arts Foundation, and a Research Grant from Nitto Foundation, a Research Grant from Takeda Science foundation, and a Research Grant from Aichi Cancer Research Foundation. A. Masuda was partly supported by Grants-in-Aid for Scientific Research (B) [Grant numbers: JP21H02476, JP21H02838], Grant-in-Aid

for Challenging Research (Exploratory) [Grant number: JP22K19269] from JSPS, and a Grant from the Japan Agency for Medical Research and Development [Grant number: JP23ek0109497]. K. Ohno was partly supported by Grants-in-Aid for Scientific Research (B) [Grant number: JP23H02794] from JSPS and Health and Labour Science Research Grant [Grant number: JP23FC1014] from the Ministry of Health Labour and Welfare. A. Mayeda was partly supported by Grants-in-Aid for Scientific Research (B) [Grant number: JP16H04705] and Grants-in-Aid for Scientific Research (C) [Grant number: JP21K06024] from JSPS.

AUTHOR COTRIBUTIONS

K. Fukumura and A. Mayeda conceived and designed the experiments; K. Fukumura performed most of the experiments and analyses, organized the data and drafted the manuscript; J.-i. Takeda and A. Masuda performed bioinformatics analyses of the sequencing data; K. Fukumura, K. Ohno and A. Mayeda revised and edited the manuscript. A. Mayeda coordinated and supervised the whole project. All authors read, corrected and approved the final manuscript.

DECLARATION of INTERESTS

The authors declare no competing interests.

REFERENCES

1. Will, C.L., and Lührmann, R. (2011). Spliceosome structure and function. Cold Spring Harb. Perspect Biol. *3*, a003707. https://doi.org/10.1101/cshperspect.a003707.
2. Kastner, B., Will, C.L., Stark, H., and Lührmann, R. (2019). Structural insights into nuclear pre-mRNA splicing in higher eukaryotes. Cold Spring Harb. Perspect. Biol. *11*, a032417. https://doi.org/10.1101/cshperspect.a032417.
3. Mayeda, A., Badolato, J., Kobayashi, R., Zhang, M.Q., Gardiner, E.M., and Krainer, A.R. (1999). Purification and characterization of human RNPS1: a general activator of pre-mRNA splicing. EMBO J. *18*, 4560-4570. https://doi.org/10.1093/emboj/18.16.4560.
4. Sakashita, E., Tatsumi, S., Werner, D., Endo, H., and Mayeda, A. (2004). Human RNPS1 and its associated factors: a versatile alternative pre-mRNA splicing regulator in vivo. Mol. Cell. Biol. *24*, 1174-1187. https://doi.org/10.1128/MCB.24.3.1174-1187.2004.
5. Trembley, J.H., Tatsumi, S., Sakashita, E., Loyer, P., Slaughter, C.A., Suzuki, H., Endo, H., Kidd, V.J., and Mayeda, A. (2005). Activation of pre-mRNA splicing by human RNPS1 is regulated by CK2 phosphorylation. Mol. Cell. Biol. *25*, 1446-1457. https://doi.org/10.1128/MCB.25.4.1446-1457.2005.
6. Le Hir, H., Sauliere, J., and Wang, Z. (2016). The exon junction complex as a node of post-transcriptional networks. Nat. Rev. Mol. Cell Biol. *17*, 41-54. https://doi.org/10.1038/nrm.2015.7.
7. Schlautmann, L.P., and Gehring, N.H. (2020). A Day in the Life of the Exon Junction Complex. Biomolecules *10*, 866. https://doi.org/10.3390/biom10060866.
8. Schwerk, C., Prasad, J., Degenhardt, K., Erdjument-Bromage, H., White, E., Tempst, P., Kidd, V.J., Manley, J.L., Lahti, J.M., and Reinberg, D. (2003). ASAP, a novel protein complex involved in RNA processing and apoptosis. Mol. Cell. Biol. *23*, 2981-2990. https://doi.org/10.1128/MCB.23.8.2981-2990.2003

9. Murachelli, A.G., Ebert, J., Basquin, C., Le Hir, H., and Conti, E. (2012). The structure of the ASAP core complex reveals the existence of a Pinin-containing PSAP complex. Nat. Struct. Mol. Biol. *19*, 378-386. https://doi.org/10.1038/nsmb.2242.

10. Joselin, A.P., Schulze-Osthoff, K., and Schwerk, C. (2006). Loss of Acinus inhibits oligonucleosomal DNA fragmentation but not chromatin condensation during apoptosis. J. Biol. Chem. *281*, 12475-12484. https://doi.org/10.1074/jbc.M509859200.

11. Barrett, S.P., Wang, P.L., and Salzman, J. (2015). Circular RNA biogenesis can proceed through an exon-containing lariat precursor. Elife *4*, e07540. https://doi.org/10.7554/eLife.07540.

12. Rodor, J., Pan, Q., Blencowe, B.J., Eyras, E., and Caceres, J.F. (2016). The RNA-binding profile of Acinus, a peripheral component of the exon junction complex, reveals its role in splicing regulation. RNA *22*, 1411-1426. https://doi.org/10.1261/rna.057158.116.

13. Wang, P., Lou, P.J., Leu, S., and Ouyang, P. (2002). Modulation of alternative pre-mRNA splicing in vivo by pinin. Biochem. Biophys. Res. Commun. *294*, 448-455. https://doi.org/10.1016/S0006-291X(02)00495-3.

14. Wang, Z., Ballut, L., Barbosa, I., and Le Hir, H. (2018). Exon Junction Complexes can have distinct functional flavours to regulate specific splicing events. Scientific reports *8*, 9509. https://doi.org/10.1038/s41598-018-27826-y.

15. Otani, Y., Fujita, K.I., Kameyama, T., and Mayeda, A. (2021). The Exon Junction Complex Core Represses Cancer-Specific Mature mRNA Re-splicing: A Potential Key Role in Terminating Splicing. Int. J. Mol. Sci. *22*, 6519. https://doi.org/10.3390/ijms22126519.

16. Krenn, V., and Musacchio, A. (2015). The Aurora B kinase in chromosome bi-orientation and spindle checkpoint signaling. Front. Oncol. *5*, 225. https://doi.org/10.3389/fonc.2015.00225.

17. Fukumura, K., Wakabayashi, S., Kataoka, N., Sakamoto, H., Suzuki, Y., Nakai, K., Mayeda, A., and Inoue, K. (2016). The exon junction complex controls the efficient and faithful splicing of a subset of transcripts involved in mitotic cell-cycle progression. Int. J. Mol. Sci. *17*, 1153. https://doi.org/10.3390/ijms17081153.

18. Fukumura, K., Inoue, K., and Mayeda, A. (2018). Splicing activator RNPS1 suppresses errors in pre-mRNA splicing: A key factor for mRNA quality control. Biochem. Biophys. Res. Commun. *496*, 921-926. https://doi.org/10.1016/j.bbrc.2018.01.120.

19. Dominguez, D., Tsai, Y.H., Weatheritt, R., Wang, Y., Blencowe, B.J., and Wang, Z. (2016). An extensive program of periodic alternative splicing linked to cell cycle progression. Elife *5*, e10288. https://doi.org/10.7554/eLife.10288.

20. Honda, R., Korner, R., and Nigg, E.A. (2003). Exploring the functional interactions between Aurora B, INCENP, and survivin in mitosis. Mol. Biol. Cell *14*, 3325-3341. https://doi.org/10.1091/mbc.E02-11-0769.

21. Badolato, J., Gardiner, E., Morrison, N., and Eisman, J. (1995). Identification and characterisation of a novel human RNA-binding protein. Gene *166*, 323-327. https://doi.org/10.1016/0378-1119(95)00571-4

22. Gilberto, S., and Peter, M. (2017). Dynamic ubiquitin signaling in cell cycle regulation. J. Cell Biol. *216*, 2259-2271. https://doi.org/10.1083/jcb.201703170.

23. Kwon, S.K., Kim, E.H., and Baek, K.H. (2017). RNPS1 is modulated by ubiquitin-specific protease 4. FEBS Lett. *591*, 369-381. https://doi.org/10.1002/1873-3468.12531.

24. Boehm, V., Britto-Borges, T., Steckelberg, A.L., Singh, K.K., Gerbracht, J.V., Gueney, E., Blazquez, L., Altmuller, J., Dieterich, C., and Gehring, N.H. (2018). Exon Junction Complexes Suppress Spurious Splice Sites to Safeguard Transcriptome Integrity. Mol. Cell *72*, 482-495. https://doi.org/10.1016/j.molcel.2018.08.030.

25. Blazquez, L., Emmett, W., Faraway, R., Pineda, J.M.B., Bajew, S., Gohr, A., Haberman, N., Sibley, C.R., Bradley, R.K., Irimia, M., and Ule, J. (2018). Exon Junction Complex Shapes the Transcriptome by Repressing Recursive Splicing. Mol. Cell *72*, 496-509. https://doi.org/10.1016/j.molcel.2018.09.033.

26. Ishigaki, Y., Nakamura, Y., Tatsuno, T., Hashimoto, M., Shimasaki, T., Iwabuchi, K., and Tomosugi, N. (2013). Depletion of RNA-binding protein RBM8A (Y14) causes cell cycle deficiency and apoptosis in human cells. Exp. Biol. Med. (Maywood) *238*, 889-897. https://doi.org/10.1177/1535370213494646.

27. Silver, D.L., Watkins-Chow, D.E., Schreck, K.C., Pierfelice, T.J., Larson, D.M., Burnetti, A.J., Liaw, H.J., Myung, K., Walsh, C.A., Gaiano, N., and Pavan, W.J. (2010). The exon junction complex component Magoh controls brain size by regulating neural stem cell division. Nat. Neurosci. *13*, 551-558. https://doi.org/10.1038/nn.2527.

28. Jang, S.W., Yang, S.J., Ehlen, A., Dong, S., Khoury, H., Chen, J., Persson, J.L., and Ye, K. (2008). Serine/arginine protein-specific kinase 2 promotes leukemia cell proliferation by phosphorylating acinus and regulating cyclin A1. Cancer Res. *68*, 4559-4570. https://doi.org/10.1158/0008-5472.CAN-08-0021.

29. Puig, O., Bragado-Nilsson, E., Koski, T., and Seraphin, B. (2007). The U1 snRNP-associated factor Luc7p affects 5' splice site selection in yeast and human. Nucleic Acids Res. *35*, 5874-5885. https://doi.org/10.1093/nar/gkm505.

30. Daniels, N.J., Hershberger, C.E., Gu, X., Schueger, C., DiPasquale, W.M., Brick, J., Saunthararajah, Y., Maciejewski, J.P., and Padgett, R.A. (2021). Functional analyses of human LUC7-like proteins involved in splicing regulation and myeloid neoplasms. Cell Rep *35*, 108989. https://doi.org/10.1016/j.celrep.2021.108989.

31. Fukumura, K., Yoshimoto, R., Sperotto, L., Kang, H.S., Hirose, T., Inoue, K., Sattler, M., and Mayeda, A. (2021). SPF45/RBM17-dependent, but not U2AF-dependent, splicing in a distinct subset of human short introns. Nat. Commun. *12*, 4910. https://doi.org/10.1038/s41467-021-24879-y.

32. Bolger, A.M., Lohse, M., and Usadel, B. (2014). Trimmomatic: a flexible trimmer for Illumina sequence data. Bioinformatics *30*, 2114-2120. https://doi.org/10.1093/bioinformatics/btu170.

33. Kim, D., Pertea, G., Trapnell, C., Pimentel, H., Kelley, R., and Salzberg, S.L. (2013). TopHat2: accurate alignment of transcriptomes in the presence of insertions, deletions and gene fusions. Genome biology *14*, R36. https://doi.org/10.1186/gb-2013-14-4-r36.

34. Trapnell, C., Hendrickson, D.G., Sauvageau, M., Goff, L., Rinn, J.L., and Pachter, L. (2013). Differential analysis of gene regulation at transcript resolution with RNA-seq. Nat. Biotechnol. *31*, 46-53. https://doi.org/10.1038/nbt.2450.

35. Katz, Y., Wang, E.T., Airoldi, E.M., and Burge, C.B. (2010). Analysis and design of RNA sequencing experiments for identifying isoform regulation. Nat. Methods *7*, 1009-1015. https://doi.org/10.1038/nmeth.1528.

36. Masuda, A., Takeda, J., Okuno, T., Okamoto, T., Ohkawara, B., Ito, M., Ishigaki, S., Sobue, G., and Ohno, K. (2015). Position-specific binding of FUS to nascent RNA regulates mRNA length. Genes Dev. *29*, 1045-1057. https://doi.org/10.1101/gad.255737.114.

FIGURES

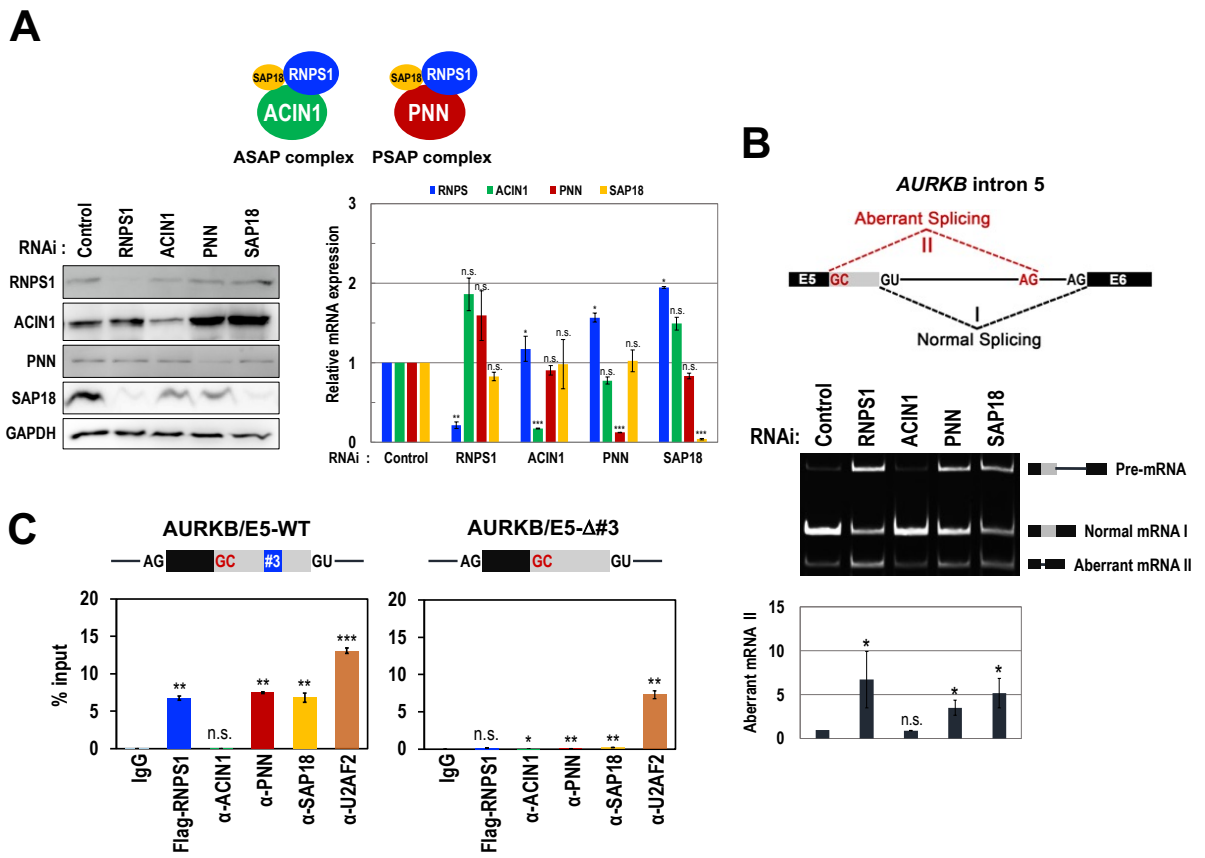

Figure 1. PSAP component binds to a specific site that is critical to promote normal splicing of the *AURKB* pre-mRNA

(A) The indicated ASAP/PSAP components were effectively depleted by RNAi-mediated knockdown in HeLa cells. These proteins were analyzed by Western blotting with indicated antibodies (left panel). These mRNA levels were analyzed by RT–qPCR using specific primer sets (right panel). Means ± standard errors (SE) are given for three independent experiments and Welch's t test values were calculated (*p < 0.05, **p < 0.005, ***p < 0.0005, n.s. p > 0.05).

(B) RNAi-mediated depletion of PSAP proteins induces splicing defect and aberrant splicing in *AURKB* pre-mRNA. Splicing products from the endogenous *AURKB* gene were detected by RT–PCR and visualized by PAGE. The bands on the PAGE gel were quantified. The ratios of the aberrantly spliced mRNA value (II) to the sum of the spliced mRNAs value (I+II) were standardized to that of the control RNAi and plotted. See (A) for the statistical analysis (*p < 0.05, n.s. p > 0.05).

(C) The PSAP, but not ASAP complex, binds to specific *cis*-element #3 in the *AURKB* exon 5. An RNA immunoprecipitation assay was performed using HeLa cells co-transfected with Flag-RNPS1 expression plasmids and the indicated AURKB-Exon 5 reporter mini-genes (WT or Δ#3). After Immunoprecipitation using the indicated antibodies, immunoprecipitated RNAs were quantified by RT–qPCR using specific primers. See (A) for the statistical analysis (*p < 0.05, **p < 0.005, ***p < 0.0005, n.s. p > 0.05).

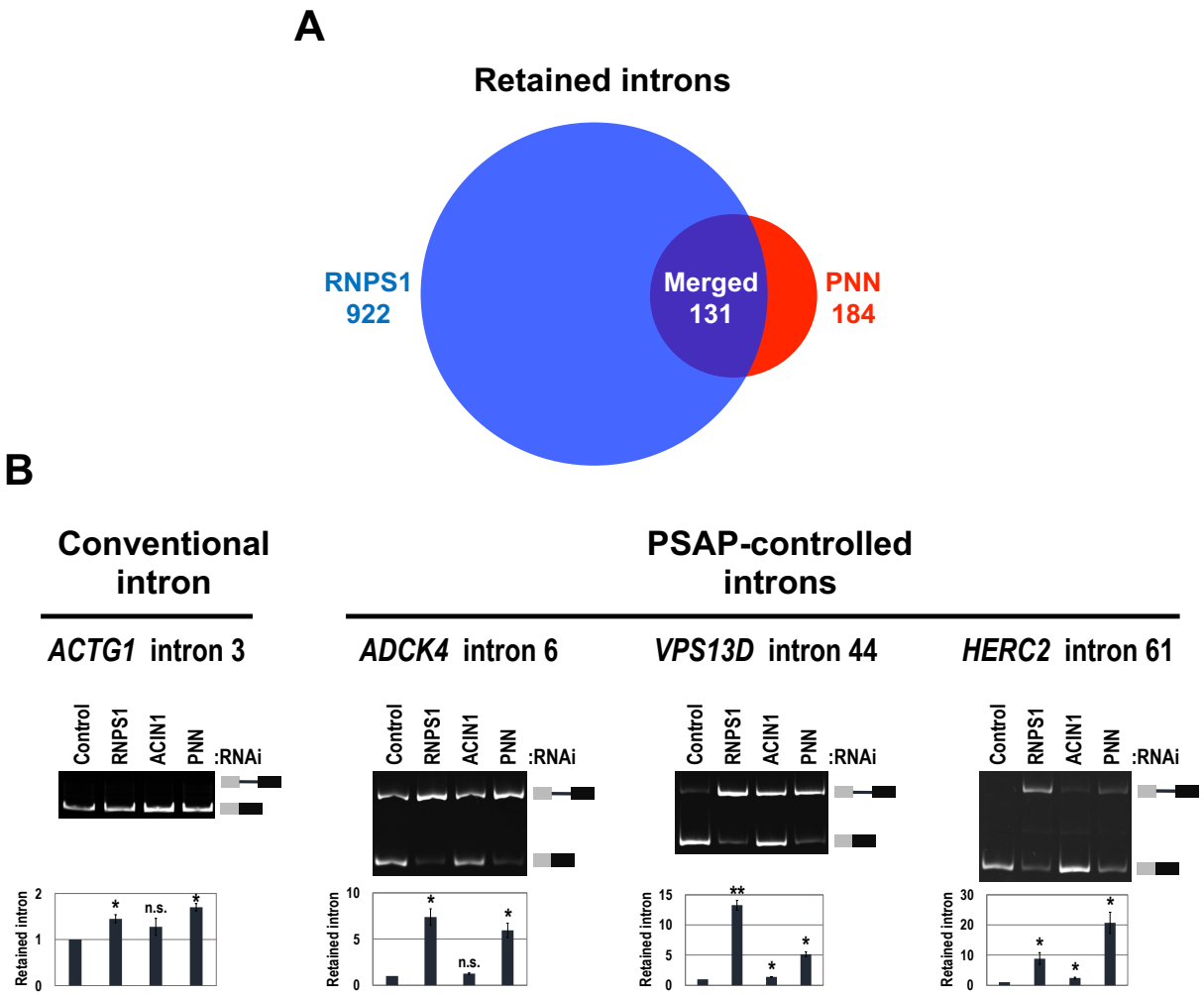

Figure 2. RNPS1 and PNN are generally required for the splicing in individual subsets of introns
(A) Venn diagram for retained introns that are generated by RNPS1- and PNN-knockdown HEK293 cells. (B) *In cellulo* splicing assays of the pre-mRNA including three representative PSAP-controlled introns and a conventional intron. After the indicated RNAi-mediated knockdown in HEK293 cells, endogenous splicing was analyzed by RT–PCR followed by PAGE (upper gel). The retained intron products were quantitated by RT–qPCR and the standardized values were plotted (lower graph). Means ± SE are given for three independent experiments and Welch's t test values were calculated (*$p < 0.05$, **$p < 0.005$, n.s. $p > 0.05$).

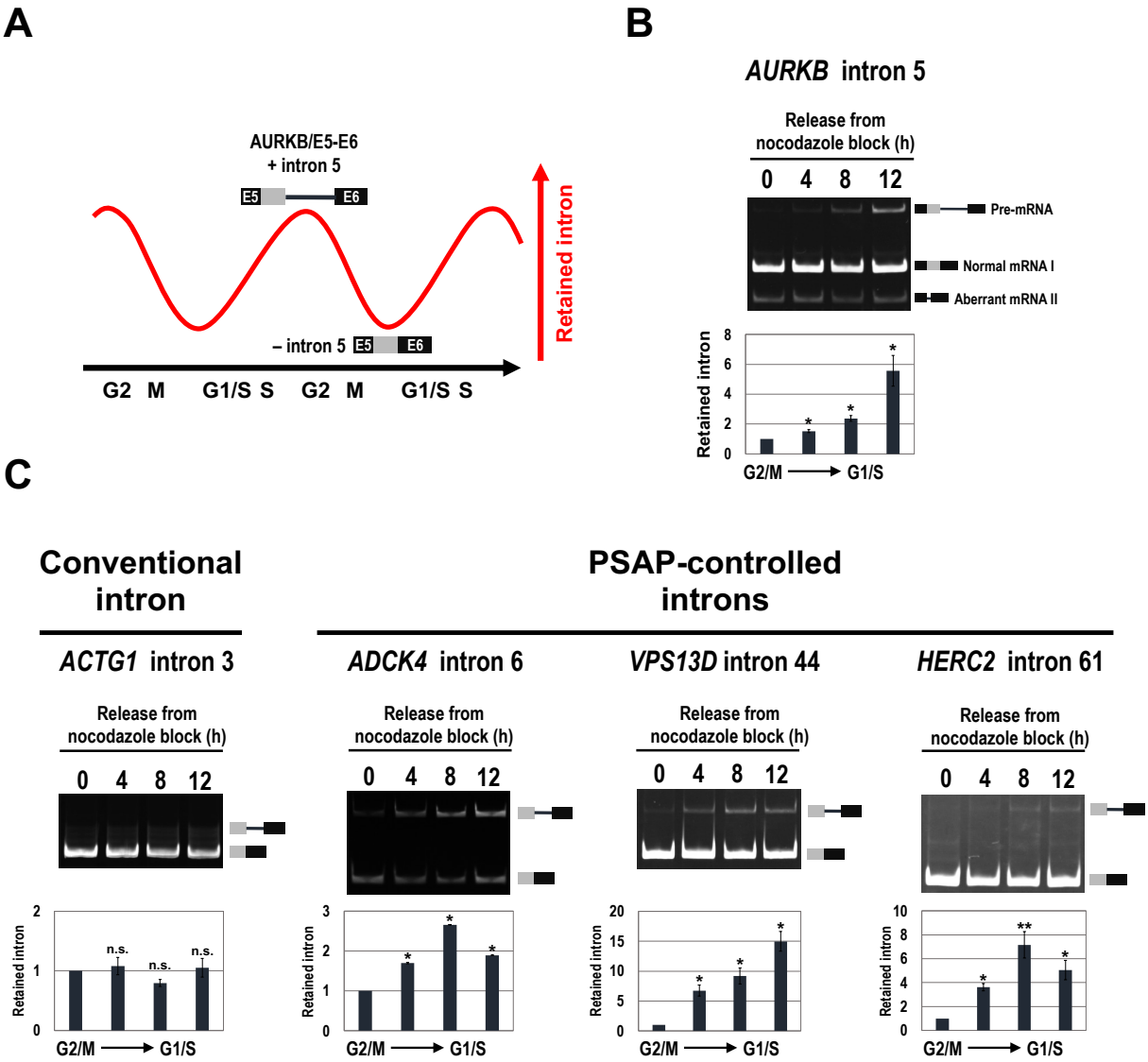

Figure 3. PSAP modulates periodic intron retention during the cell cycle from G2/M to G1/S phase

(A) Schematic representation of cyclical retention of *AURKB* intron 5 (modified from Ref.[19]).

(B) Periodic *AURKB* intron 5 retention across the cell cycle is recapitulated in our splicing assays *in cellulo*. HEK293 cells were synchronized in G2/M phase by treating with nocodazole, washed, released, and harvested at the indicating time points. The endogenous splicing of *AURKB* intron 5 was analyzed by RT–PCR followed by PAGE (upper gel). The retained intron products (pre-mRNAs) were quantitated by RT–qPCR, and the retained intron values were standardized to that at the start time, 0 h (lower graph). A trace level of aberrantly spliced product (II), which was not changed across the cell cycle, was due to the toxicity of nocodazole. Means ± SE are given for three independent experiments and Welch's t test values were calculated (*$p < 0.05$).

(C) Periodic intron retention across the cell cycle was observed in three representative PSAP-controlled introns. Synchronized experiments with HEK293 cells, endogenous splicing assays, quantification and the statistical analysis were performed as described in (B) (*$p < 0.05$, **$p < 0.005$, n.s. $p > 0.05$).

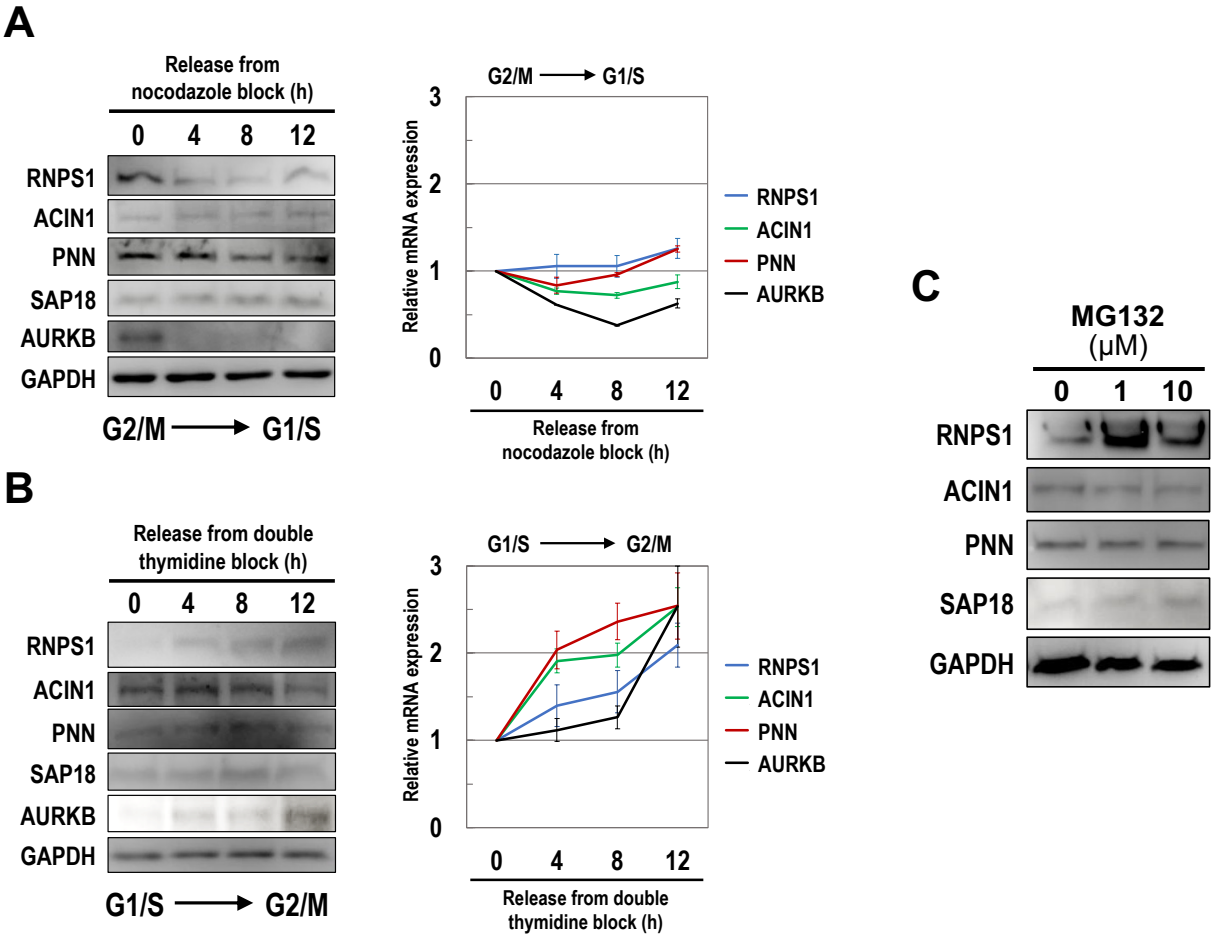

Figure 4. RNPS1 protein level is coordinated with AURKB protein level during the cell cycle, in which the ubiquitin-proteasome pathway plays a critical role

(A) Expression level of RNPS1 protein, but not all other ASAP and PSAP proteins, decreases from G2/M to G1/S phase. HEK293 cells were synchronized in G2/M phase by nocodazole and released cells were harvested at indicated time points. Total proteins were analyzed by Western blotting with indicated antibodies (left panel). mRNA levels were analyzed by RT–qPCR and the relative values were standardized to that at the start time, 0 h (right graph). Means ± SE are given for three independent RT–qPCR experiments.

(B) Expression level of RNPS1 protein, but not all other ASAP and PSAP proteins, increases from G1/S to G2/M phase. HEK293 cells were synchronized at G1/S phase by double thymidine block and total proteins and mRNAs were analyzed as described in (A). See (A) for the statistical analysis.

(C) The protein levels of the indicated PSAP/ASAP components in the presence of proteasome inhibitor MG132. A common solvent, dimethyl sulfoxide (DMSO), was added in 0 μM. HEK293 cells were cultured for 24 h with the indicated concentration of MG132 and the protein levels were analyzed by Western blotting using the antibody against each protein.

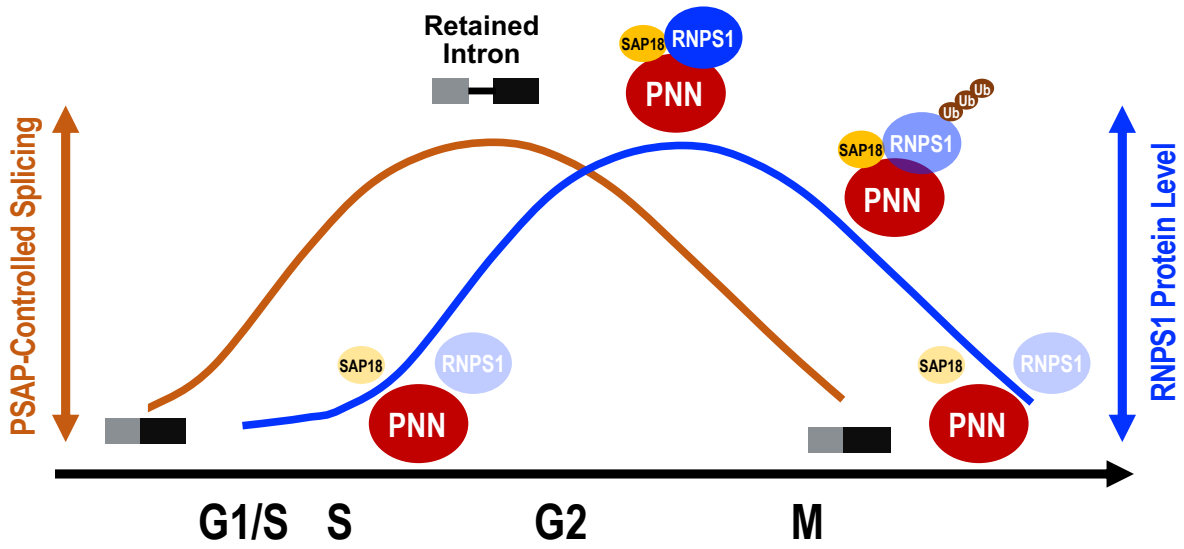

Figure 5. The model of RNPS1-mediated periodic modulation of splicing during cell cycle
We discovered that RNPS1 protein, but neither PNN nor SAP18 protein, in PSAP plays an essential role to control periodic splicing over the cell cycle progression. The ubiquitin-mediated proteolysis of RNPS1 also destabilizes SAP18, leading to the dissociation of PSAP complex.

Article

RNPS1 in PSAP complex controls periodic pre-mRNA splicing over the cell cycle

Kazuhiro Fukumura[1,*], Akio Masuda[2], Jun-ichi Takeda[2], Kinji Ohno[2] and Akila Mayeda[1,5,*]

[1]Division of Gene Expression Mechanism, Center for Medical Science, Fujita Health University, Toyoake, Aichi 470-1192, Japan

[2]Division of Neurogenetics, Center for Neurological Disease and Cancer, Nagoya University Graduate School of Medicine, Nagoya, Aichi 466-8550, Japan

[5]Lead Contact

*Correspondence:
fukumura@fujita-hu.ac.jp (K.F.), mayeda@fujita-hu.ac.jp (A.M.)

Contents

Table S1

Figure S1

Figure S2

Figure S3

Figure S4

SUPPLEMENTARY REFERENCES

Tables S2
(Uploaded in the separate Excel file)

Table S1 List of all the synthetic oligonucleotides used in the experiments

siRNAs (sense sequences) for cellular knockdown (*T*: deoxyribonucleotide)		
RNPS1-siRNA	5′-GCAAAGACCGCUCAGAUGA*TT*-3′	Knockdown of *RNPS1*
ACIN1-siRNA	5′-GAGGCCUUCUGGAUUGACA*TT*-3′	Knockdown of *ACIN1*
PNN-siRNA	5′-GAAGGUAGACGCAUCGAAU*TT*-3′	Knockdown of *PNN*
SAP18-siRNA	5′-CCAGCGAGUUGCAGAUCUA*TT*-3′	Knockdown of *SAP18*
GPATCH8-siRNA	5′-GACCAGAGCUGCUAUAGUA*TT*-3′	Knockdown of *GPATCH8*
LUC7L3-siRNA	5′-GAAGUAGAACGUAGGAUCA*TT*-3′	Knockdown of *LUC7L3*
Primer DNAs for plasmid constructions		
AURKB/I4-E5-I5-F	5′-CAGTGTGCTGGAATTGTTCTGAGTTGCCTTCCTC-3′	Construction of pcDNA3-AURKB/E5-WT & pcDNA3-AURKB/E5-Δ#3
AURKB/I4-E5-I5-R	5′-TAGATGCATGCTCGAGGCTTCGGCTCAGGGGGC-3′	
AURKB/E5/inR-E6-F1	5′-GAAATCCAGGCCCACAAGTCCCAGATAGAG-3′	Construction of pcDNA3-AURKB/E5/inR-E6
AURKB/E5/inR-E6-R1	5′-CAACCCATACTGCAGGTGGGCCTGGATTTC-3′	
AURKB/E5/inR-E6-F2	5′-GAAATCCAGGCCCACCTGCAGTATGGGTTG-3′	
AURKB/E5/inR-E6-R2	5′-CTCTATCTGGGACTTGTGGGCCTGGATTTC-3′	
AURKB/E5/inL-E6-F1	5′-AAGAAAAGCCATTTCATAAGTCCCAGATAGAGAA-3′	Construction of pcDNA3-AURKB/E5/inL-E6
AURKB/E5/inL-E6-R1	5′-GGACCTTGAGCGCCACGGTGGGCCTGGATTTCGA-3′	
AURKB/E5/inL-E6-F2	5′-TCGAAATCCAGGCCCACCGTGGCGCTCAAGGTCC-3′	
AURKB/E5/inL-E6-R2	5′-TTCTCTATCTGGGACTTATGAAATGGCTTTTCTT-3′	
Primer DNAs for assays		
AURKB/E5-F	5′-GGAATTCCGGCGGCACTTCACAATTGATG-3′	Splicing assay of endogenous *AURKB* intron 5
AURKB/E6-R	5′-CCGCTCGAGGCTGTTCGCTGCTCGTCAA-3′	
MDM2/E8-F	5′-CTTTGATGAAAGCCTGGCTC-3′	Splicing assay of endogenous *MDM2* intron 9
MDM2/E10-R	5′-CCTGCCTGATACACAGTAACT-3′	
RNPS1-PCR-F	5′-GAAGCACATGGATGGAGGAC-3′	PCR & qPCR detections of endogenous *RNPS1* mRNA
RNPS1-PCR-R	5′-GGAGACCTGCGCCACATA-3′	
ACIN1-PCR-F	5′-GCAGACCAAGTCAGCAATGA-3′	PCR & qPCR detections of endogenous *ACIN1* mRNA
ACIN1-PCR-R	5′-CCCCCTCTGTGTCACTGTTT-3′	
PNN-PCR-F	5′-AGAAGAGAATCACGCCAGGA-3′	PCR & qPCR detections of endogenous *PNN* mRNA
PNN-PCR-R	5′-CCGCTTTTGCCTTTCAGTAG-3′	
SAP18-PCR-F	5′-ATGCTCGCTGCAGGGGTC-3′	qPCR detection of endogenous *SAP18* mRNA
SAP18-PCR-R	5′-TTAATATGGTCTCATGCGCCCT-3′	
GPATCH8-PCR-F	5′-CTTCAGGGTCTGCCTGTAGC-3′	PCR detection of endogenous *GPATCH8* mRNA
GPATCH8-PCR-R	5′-GTTTTCGTTTCTTGCGCTTC-3′	

LUC7L3-PCR-F	5′-CTCAAGCCGAACATCAGACA-3′	PCR detection of endogenous *LUC7L3* mRNA
LUC7L3-PCR-R	5′-CTCTGTCCCGACTTTTGCTC-3′	
ACTG1-PCR-F	5′-CCCATCTACGAGGGCTACG-3′	PCR & qPCR detections of endogenous *ACTG1* mRNA
ACTG1-PCR-R	5′-TTCATGAGGTAGTCGGTCAGG-3′	
AURKB-PCR-F	5′-CTCCTACCCCTGGCCCTA-3′	qPCR detection of endogenous *AURKB* mRNA
AURKB-PCR-R	5′-GATGGGGTGACAGGCTCTT-3′	
T7	5′-AATACGACTCACTATAG-3′	RIP assay for *AURKB*/E5-WT and *AURKB*/E5Δ#3 reporter
AURKB/E6-R	5′-CCGCTCGAGGCTGTTCGCTGCTCGTCAA-3′	
ACTG1/E3-F	5′-TGACCCTGAAGTACCCCATT-3′	Splicing assay of endogenous *ACTG1* intron 3
ACTG1/E4-R	5′-TGGTGGTGAAGCTGTAGCCT-3′	
ADCK4/E6-F	5′-AATGCCGAGCGGATTGTG-3′	Splicing assay of endogenous *ADCK4* intron 6
ADCK/E7-R	5′-GGACCCGCTCAAAGATGTG-3′	
VPS13D/E44-F	5′-TCTCTTCACTCCCACCAGTG-3′	Splicing assay of endogenous *VPS13D* intron 44
VPS13D/E45-R	5′-GTGTCCATAGAGTGGCACTCT-3′	
HERC2/E61-F	5′-ACTGTGACAAACCAAGGCTG-3′	Splicing assay of endogenous *HERC2* intron 61
HERC2/E62-R	5′-CTTCATCGGTCAGAGCCAG-3′	
AURKB/spliced-F	5′-CAGGCCCACCTGCACCAT-3′	qPCR detection of endogenous *AURKB* spliced mRNA
AURKB/E6-R	5′-CCGCTCGAGGCTGTTCGCTGCTCGTCAA-3′	
AURKB/I5-F	5′-AGTGAGCCCCTTTAGCTCTT-3′	qPCR detection of endogenous *AURKB* intron 5 retained mRNA
AURKB/I5-R	5′-TGGGAGTGGTAAGGGGAAA-3′	
ADCK4/spliced-F	5′-AGATGCTCAGCATCCAGGAC-3′	qPCR detection of endogenous *ADCK4* spliced mRNA
ADCK4/E7-R	5′-GGACCCGCTCAAAGATGTG-3′	
ADCK4/E6-F	5′-AATGCCGAGCGGATTGTG-3′	qPCR detection of endogenous *ADCK4* intron 6 retained mRNA
ADCK4/I6-R	5′-GAGTCGAGGGTCATGCTGTA-3′	
VPS13D/spliced-F	5′-ATCAGCTCCAGACAAGCCAG-3′	qPCR detection of endogenous *VPS13D* spliced mRNA
VPS13D/E45-R	5′-GTGTCCATAGAGTGGCACTCT-3′	
VPS13D/I44-F	5′-GAGGACCATTGCCTGAAAGTG-3′	qPCR detection of endogenous *VPS13D* intron 44 retained mRNA
VPS13D/E45-R	5′-GTGTCCATAGAGTGGCACTCT-3′	
HERC2/E61-F	5′-ACTGTGACAAACCAAGGCTG-3′	qPCR detection of endogenous *HERC2* spliced mRNA
HERC2/spliced-R	5′-GACCGAGAAGGACTTTCACCA-3′	
HERC2/I61-F	5′-TGCCTGTGCGTGATTCTG-3′	qPCR detection of endogenous *HERC2* intron 61 retained mRNA
HERC2/E62-R	5′-CTTCATCGGTCAGAGCCAG-3′	

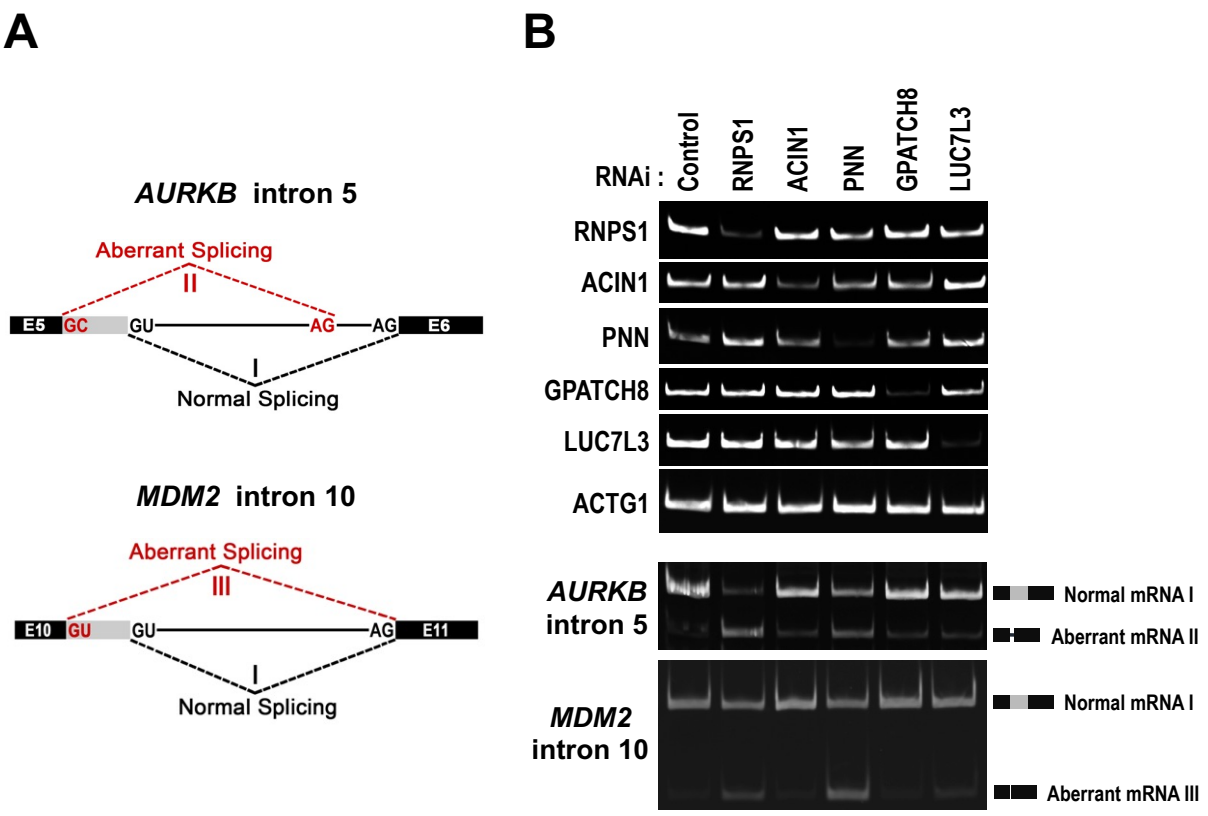

Figure S1. Knockdown of PSAP-specific component, but not ASAP-specific component and other RNPS1-binding factors, induces aberrant splicing in two PSAP-controlled pre-mRNAs

(A) Schematic diagram of pre-mRNA splicing pathways that generate the normal mRNA (I) and aberrant mRNAs (II, III) in the indicated pre-mRNA. Previously it was shown that these aberrant mRNAs (II, III) are generated by siRNA-mediated depletion of RNPS1, a component of PSAP[1].

(B) RNAi-mediated depletion of the ASAP-specific component (ACIN1) and PSAP-specific component (PNN) together with other RNPS1-binding proteins (GTATCH8 and LUC7L3) in HeLa cells and these proteins were analyzed by Western blotting with indicated antibodies (upper panel). Indicated spliced mRNAs (I, II, III) from the endogenous *AURKB* and *MDM2* genes were detected by RT–PCR and visualized by PAGE (lower panel). GPATCH8 (G patch domain-containing protein 8) was isolated from human brain cDNA library and function was unknown. Previous exome sequencing study showed that a mutation in GPATCH8 associated with hyperuricemia co-segregating with osteogenesis imperfecta[2]. LUC7L3 (LUC7 like3) is a homolog of yeast U1 snRNP component LUC7, which is involved in alternative splicing regulation in human[3,4].

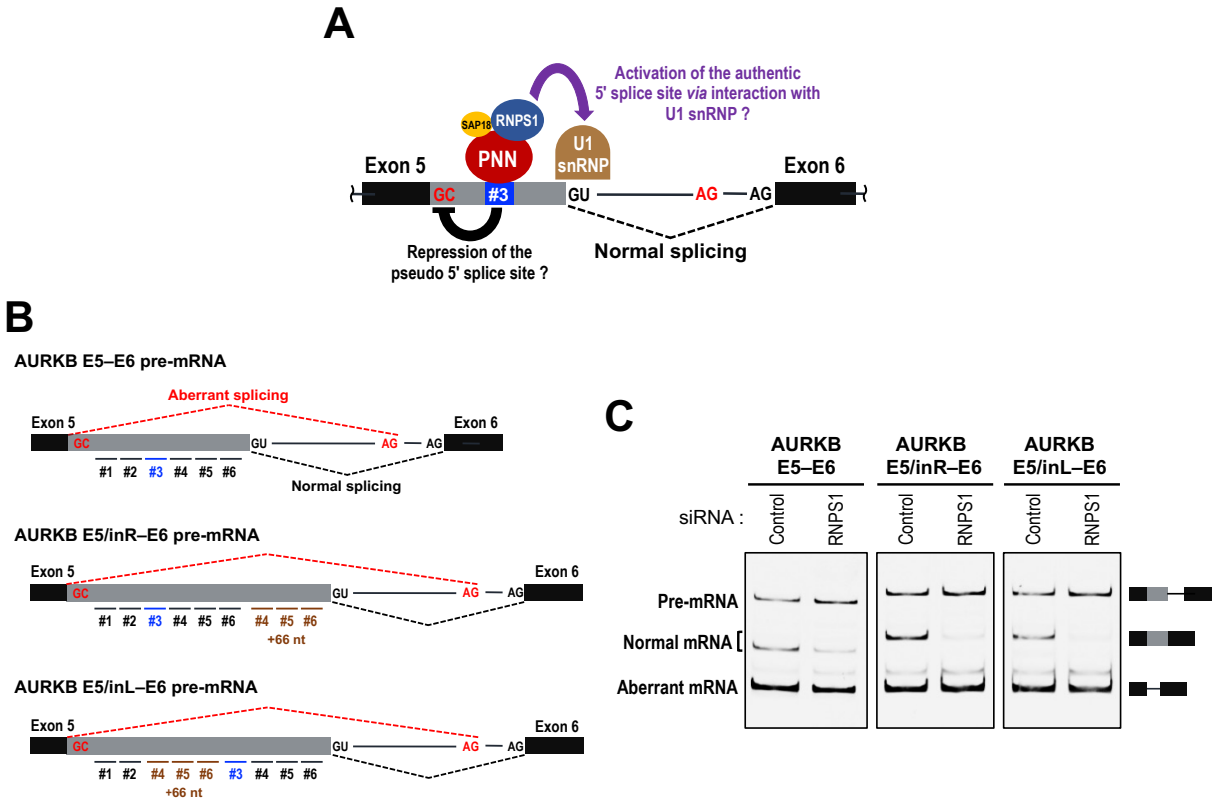

Figure S2. PSAP either represses the upstream pseudo 5′ splice site or activates the downstream authentic 5′ splice site to ensure precise splicing of *AURKB* pre-mRNA

(A) Schematic diagram of two possible PSAP-mediated mechanisms to maintain normal splicing. (i) PSAP on the target site (#3) can repress the upstream pseudo 5' splice site through either direct masking or indirect interference. (ii) PSAP on the target site (#3) can activate the downstream authentic 5' splice site through RNPS1 interaction with a component of U1 snRNP[1].

(B) Three *AURKB* mini-gene transcripts to test the above models. The distances from PSAP-binding site (#4) to either upstream authentic 5' splice site or downstream pseudo 5' splice site were expanded by inserted duplicated fragment (#4-#5-#6) in E5/inR–E6 and E5/inL–E6 mini-genes, respectively.

(C) *In cellulo* splicing assay of ectopically expressed these three *AURKB* mini-genes. Splicing products were detected by RT–PCR using specific primer sets and visualized by PAGE. Normal and aberrant mRNA products, depicted in (B), are shown schematically at the right side.

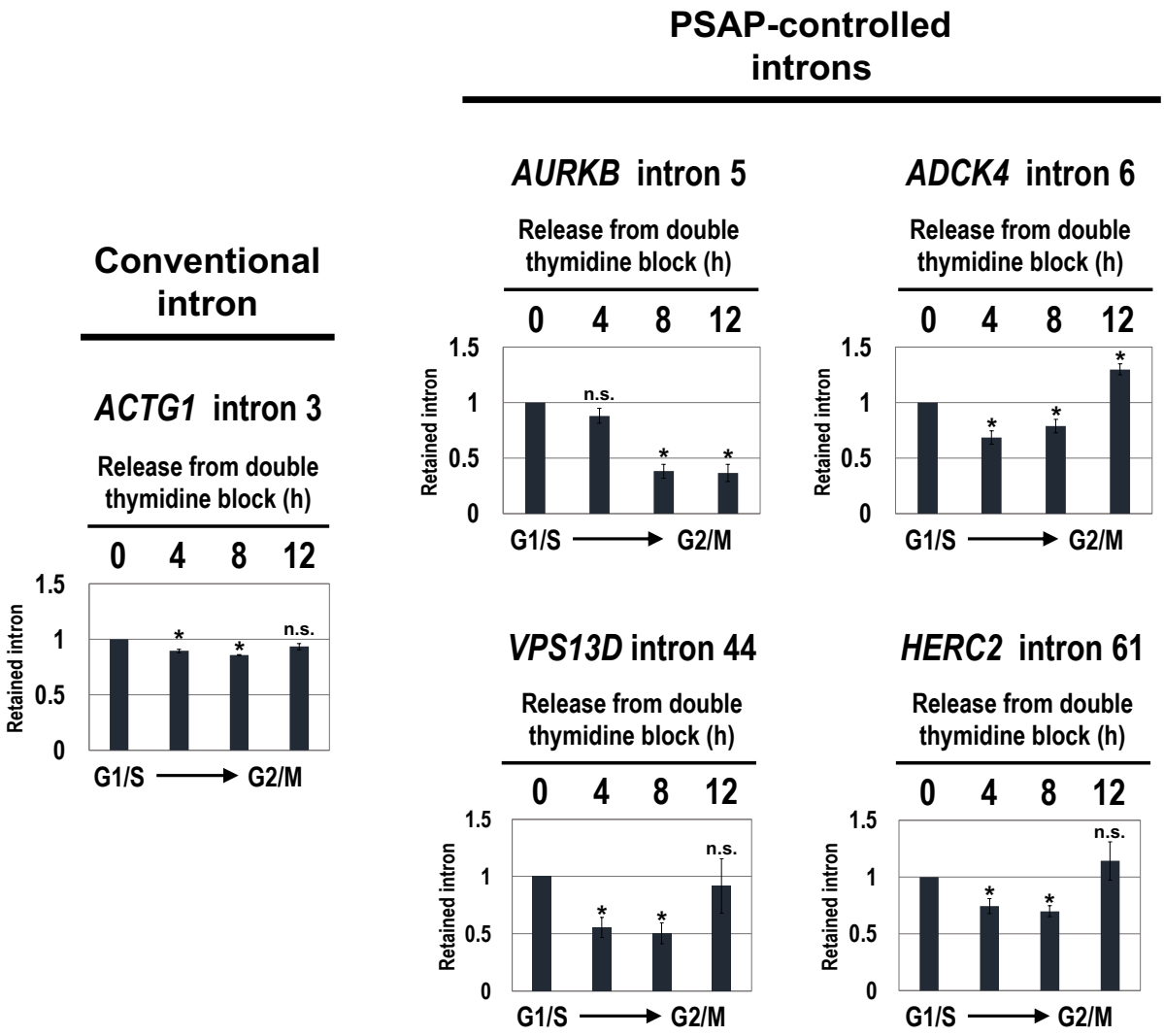

Figure S3. PSAP modulates periodic intron retention during the cell cycle from G1/S to G2/M phase

HEK293 cells were synchronized in G1/S phase by double thymidine block, released, and harvested at the indicating time points. Endogenous splicing in the indicated introns was analyzed by RT–qPCR and the retained intron values were standardized to that at the start time, 0 h. Means ± SE are given for three independent experiments and Welch's t test values were calculated (*$p < 0.05$, n.s. $p > 0.05$).

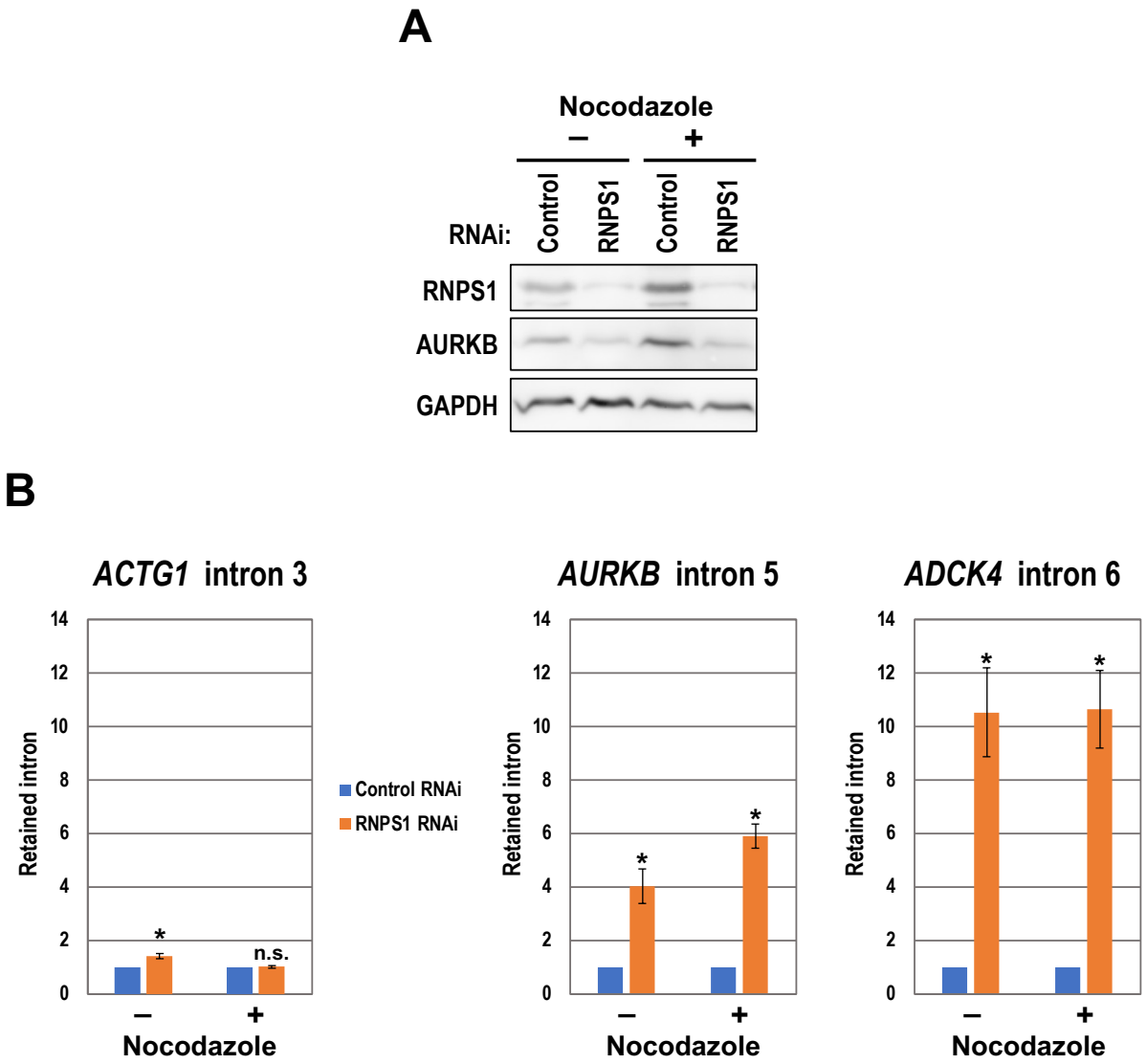

Figure S4. Knockdown of RNPS1 induces retention of PSAP-regulated introns irrespective of cell cycle phase

(A) RNPS1 was depleted by RNAi-mediated knockdown in HEK293 cells and treated with nocodazole to arrest the cell cycle at the G2/M phase. Proteins were analyzed by Western blotting with indicated antibodies. *AURKB* is downregulated by RNPS1-knockdown as previously described[1].

(B) Indicated retained introns were analyzed by RT–qPCR and the values were standardized to that of the control-knockdown and plotted. Means ± SE are given for three independent experiments and Welch's t test values were calculated (*$p < 0.05$, n.s. $p > 0.05$).

SUPPLEMENTARY REFERENCES

1. Fukumura, K., Inoue, K., and Mayeda, A. (2018). Splicing activator RNPS1 suppresses errors in pre-mRNA splicing: A key factor for mRNA quality control. Biochem. Biophys. Res. Commun. *496*, 921-926. https://doi.org/10.1016/j.bbrc.2018.01.120.

2. Kaneko, H., Kitoh, H., Matsuura, T., Masuda, A., Ito, M., Mottes, M., Rauch, F., Ishiguro, N., and Ohno, K. (2011). Hyperuricemia cosegregating with osteogenesis imperfecta is associated with a mutation in GPATCH8. Hum. Genet. *130*, 671-683. https://doi.org/10.1007/s00439-011-1006-9.

3. Fortes, P., Bilbao-Cortes, D., Fornerod, M., Rigaut, G., Raymond, W., Seraphin, B., and Mattaj, I.W. (1999). Luc7p, a novel yeast U1 snRNP protein with a role in 5' splice site recognition. Genes Dev. *13*, 2425-2438. https://doi.org/10.1101/gad.13.18.2425.

4. Gao, G., Xie, A., Huang, S.C., Zhou, A., Zhang, J., Herman, A.M., Ghassemzadeh, S., Jeong, E.M., Kasturirangan, S., Raicu, M., et al. (2011). Role of RBM25/LUC7L3 in abnormal cardiac sodium channel splicing regulation in human heart failure. Circulation *124*, 1124-1131. https://doi.org/10.1161/CIRCULATIONAHA.111.044495.